The Goodwin Oscillator: On the Importance of Degradation Reactions in the Circadian Clock

Peter Ruoff,*[,1] Merete Vinsjevik,* Christian Monnerjahn,[†] and Ludger Rensing[†]
*School of Technology and Science, Stavanger College, N-4091 Stavanger, Norway, [†]Department of Biology, University of Bremen, D-28334 Bremen, Germany

Abstract This article focuses on the Goodwin oscillator and related minimal models, which describe negative feedback schemes that are of relevance for the circadian rhythms in *Neurospora, Drosophila,* and probably also in mammals. The temperature behavior of clock mutants in *Neurospora crassa* and *Drosophila melanogaster* are well described by the Goodwin model, at least on a semi-quantitative level. A similar semi-quantitative description has been found for *Neurospora crassa* phase response curves with respect to moderate temperature pulses, heat shock pulses, and pulses of cycloheximide. A characteristic feature in the Goodwin and related models is that degradation of clock-mRNA and clock protein species plays an important role in the control of the oscillator's period. As predicted by this feature, recent experimental results from *Neurospora crassa* indicate that the clock (FRQ) protein of the long period mutant frq^7 is degraded approximately twice as slow as the corresponding wild-type protein. Quantitative RT-PCR indicates that experimental frq^7-mRNA concentrations are significantly higher than wild-type levels. The latter findings cannot be modeled by the Goodwin oscillator. Therefore, a threshold inhibition mechanism of transcription is proposed.

Key words circadian rhythms, clock mutants, temperature compensation, homeostasis, Goodwin oscillator, phase shifts, *Neurospora crassa, Drosophila*

It is now generally believed that circadian rhythms have a clock-function for timing important physiological processes with respect to daily and seasonal environmental changes (Edmunds, 1988). To work as useful chronometers, circadian oscillators compensate for environmental fluctuations, such as, for example, changes in temperature, salinity, pH, or nutrient supply, which may otherwise influence the oscillator's period and thus the temporal organization of the organism (Pittendrigh, 1993). Especially the influence of temperature on the clock has been studied extensively, and temperature compensation has been recognized to be one of the main characteristics of circadian clocks (Edmunds, 1988; Winfree, 1980). Temperature compensation means that the period of the rhythm remains practically unchanged at different environmental temperatures as long as the temperature is kept constant. Although temperature compensation ensures that the period is unaltered at different constant environmental temperatures, the *phase* of the oscillator will in general vary with (sudden) temperature changes. Also, many ultradian rhythms have been found to be temperature compensated (Kippert, 1997; Ruoff et al., 1999b).

Our work has mainly focused on the Goodwin model and its behavior to describe and predict properties of circadian rhythms. A characteristic feature of the Goodwin and related models is that degradation reactions of both clock mRNA and clock protein play an important role in the control of the oscillator's

1. To whom all correspondence should be addressed.

JOURNAL OF BIOLOGICAL RHYTHMS, Vol. 14 No. 6, December 1999 469-479

Table 1. *frq*$^+$ and *frq*^{7} parameterization in Goodwin model

Type	k_4	k_5	k_6	*Period*	*Start Values* (t = 0)
frq$^+$	0.2	0.2	0.1	22.3	$X_0 = 3.931 \times 10^{-2}$ $Y_0 = 1.811 \times 10^{-1}$ $Z_0 = 1.712$
frq^7	0.2	0.1	0.1	28.2	$X_0 = 2.214 \times 10^{-2}$ $Y_0 = 1.918 \times 10^{-1}$ $Z_0 = 1.826$

NOTE: $k_1 = k_2 = k_3 = 1.0$ in all cases.

period (Lewis, 1994; Olde Scheper et al., 1999; Ruoff and Rensing, 1996; Ruoff et al., 1996; Ruoff et al., 1999). As predicted by this feature, recent experimental results from *Neurospora crassa* show that the clock (FRQ) protein of the long period mutant *frq*^{7} is degraded approximately twice as slow as the corresponding wild-type protein. Quantitative RT-PCR indicates that *frq*^{7}-mRNA levels are significantly higher than wild-type levels. The latter findings, however, cannot be described by the original Goodwin model, and therefore an alternative inhibition mechanism is introduced and discussed.

MATERIALS AND METHODS

Computations

The differential equation from the models were solved numerically on a Macintosh PowerPC or HP9000 computer using the double-precision version of the FORTRAN subroutine LSODE (Hindmarsh, 1980). Phase response curves (PRCs) were calculated relative to the *X* (*frq*-mRNA)-maxima, which for free-running conditions was set to circadian time (CT) 0 (Aronson et al., 1994). We have mainly described the *Neurospora crassa* wild-type (*frq*$^+$) and the long period mutant *frq*^{7} mutant by the Goodwin model. The rate constants values for the *frq*$^+$ and *frq*^{7} parameterizations are given in Table 1.

Nonlinear curve fitting has been performed by the Macintosh version of the program Kaleidagraph (Synergy Software, 1997).

Quantitative RT-PCR

Left and right primers *frqfor*1 (agaagaagctggttgtc cga) and *frqrev*1 (tccgaccattcttatccgag) were constructed using the primer construction program PRIMER3 (http://www-genome.wi.mit.edu/cgi-bin/primer/primer3.cgi). Primer sequences were checked to avoid possible hairpin loops. The *frq* PCR product size is 747 bp.

Total RNA was extracted from 10 mg mycel using a commercial extraction kit (Purescript®, Gentra Systems). The RNA was treated with DNase I (10 min at 37° C and 5 min at 65° C). The final RNA solution was stored at –30° C.

19 µL of RT reaction solution containing 1.25 µL 10 mM dNTP, 1 µg total RNA was kept for 5 min at 70° C and then cooled on ice. Then 5 µL *frqrev*1 (10 pmol/µL) and 1 µL of M-MLV Reverse Transcriptase (200 units) were added. The reaction solution was kept at 42° C for 60 min. Finally, the solution was heated to 70° C for 10 min and then kept at 4° C for subsequential use in the PCR.

The PCR was performed in a Perkin-Elmer GeneAmp PCR System 2400. One µL of RT reaction solution from above was used in the PCR process with a reaction volume of 50 µL. Two units of PLATINUM® *Taq* DNA polymerase (Gibco) was applied. The reaction buffer was 20 mM Tris-HCl, pH 8.4 with 50 mM KCl, 1.5 mM $MgCl_2$, 200 µM dNTPs, and 40 pmol of *frqfor*1 and *frqrev*1, respectively. The PCR temperature profile was {94° C (2 min)} – {94° C (30 s), 65° C (30 s), 72° C (45 s)}$_{5cycles}$ – {94° C (30 s), 62° C (30 s), 72° C (45 s)}$_{5cycles}$ – {94° C (30 s), 60° C (30 s), 72° C (45 s)}$_{25cycles}$ – {72° C (7 min)} – {4° C (storage)}. PCR products were fluorimetrically detected by electrophoresis with UV-illumination of gels that contained ethidium bromide. The gels consisted of 1.2% ultrapure agarose (Gibco) and 10 µg ethidium bromide in 100 mL gel.

For quantification, a purified 536 bp DNA fragment "MIMIC" (Siebert and Kellogg, 1995) was added at various concentrations to the PCR reaction mixture containing *frq* cDNA. MIMIC was constructed from the *N. crassa nit*-3 gene and is amplifiable with *frqfor*1 and *frqrev*1. After PCR and gel electrophoresis fluorescence intensities of the *frq* PCR product and the amplified MIMIC were compared. Photographs of gels were taken, and fluorescence intensities were measured from the photograph by using the freeware program

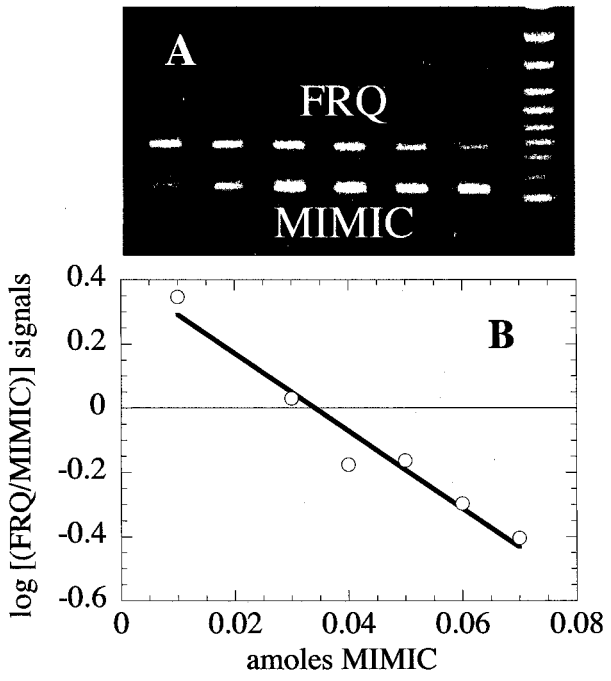

Figure 1. Estimation of *frq*-mRNA by competitive amplification with known amounts of MIMIC (amoles: 10^{-18} moles). A. Agarose gel analysis of competitive PCR with same amounts of *frq*-cDNA but varying amounts of MIMIC. B. Densitometric analysis of FRQ and MIMIC signals from A.

NIH Image (Macintosh Version 1.61, National Institutes of Health). At equal fluorescence intensities, the *frq*-cDNA concentration was assumed to be equal to the concentration of the added MIMIC (Fig. 1).

Strains and Culture Methods

The strains used were *band* (*bd*) with the wild-type *frequency* gene (*frq*$^+$) or the *frq*^{7} mutation. The *bd frq*$^+$ and the *bd frq*^{7} mutants were obtained from Fungal Genetics Stock Center (FGSC) (The University of Kansas Medical Center, Department of Microbiology, 3901 Rainbow Blvd., Kansas City, Kansas 66160-7420, USA. FGSC Stock No.: *bd*, 1858; *frq*^{7}, 4898 [Internet: http://www.kumc.edu/research/fgsc/main.html]).

Cultures were grown in liquid Vogel's medium (Vogel, 1956) with 2% sucrose (LL-medium). After inoculation of approximately 6×10^7 conidia L^{-1} in Petri dishes (90 mm diameter), they were exposed to white fluorescent light for 36 h at 25° C. Then discs were cut out (1 cm in diameter) by means of a cork borer and placed in Vogel's medium with low sucrose (0.05%) at constant darkness (DD), which corresponds to circadian time (CT) 12. It is the transition into DD conditions that initiates or sets the phase of the circadian rhythm.

TEMPERATURE COMPENSATION: GENERAL CONSIDERATIONS

All chemical change, no matter how complex, is believed to be a consequence of underlying elementary processes (Noyes, 1986). An elementary process takes place in a single step and involves at most three reactant or product molecules. Kinetic orders in each reaction direction are equal to the stoichiometric coefficients of the elementary process, and the direction of the process is determined by the affinity or free energy of the process (Kondepudi and Prigogine, 1998). Elementary processes can be grouped into sets of component stoichiometric processes, which together describe the overall change from reactants to products in a complex reaction system.

The influence of temperature on an elementary process is described by the Arrhenius equation, which connects the rate constant k_i of process i with the absolute temperature T (Laidler and Peterman, 1979):

$$k_i(T) = A_i \exp(-E_i/RT). \quad (1)$$

A_i is the so-called pre-exponential factor. In most cases, A_i can be considered to be independent of temperature. E_i is the activation energy, which can be visualized as an energy barrier the molecules have to pass to form a product. The Arrhenius equation has also been applied to chemically "unconventional" processes as, for example, to the rates of cricket chirping or firefly flashing, or even to the temperature dependence of subjective time perception in humans (Laidler, 1972).

The processes in a reaction kinetic oscillator can be grouped into period-increasing and period-decreasing reactions. For each process Ri, a rate constant k_i and a corresponding activation energy E_i can be assigned. The temperature dependence of the (assumed isothermic) oscillator's period P will be a complicated function f of the simultaneous influence of temperature T on all k_i:

$$P(T) = f\{k_1(T), k_2(T), \ldots, k_i(T), \ldots\}. \quad (2)$$

The temperature dependence of P can be written as

$$\frac{\partial P}{\partial T} = \sum_i \left(\frac{\partial f}{\partial k_i}\right)\left(\frac{\partial k_i}{\partial T}\right). \quad (3)$$

Temperature compensation requires that $\partial P/\partial T = 0$. By including the Arrhenius equation into equation 3, one gets a condition for temperature compensation ("antagonistic balance in temperature") that is valid for any *reaction kinetic* oscillator (Ruoff, 1992):

$$\sum_{j(P\text{-increasing})} \left(\frac{\partial \ln(f)}{\partial \ln(k_j)}\right) \times E_j = - \sum_{i(P\text{-increasing})} \left(\frac{\partial \ln(f)}{\partial \ln(k_i)}\right) \times E_i . \quad (4)$$

In other words, in any reaction kinetic oscillator, temperature compensation is expected to occur whenever the E_i-weighted sum of $\partial \ln f/\partial \ln k_i$ of period-increasing reactions balance the corresponding negative sum of period-decreasing reactions. Equation 4 may be considered as a generalization of the principle of "opposing reactions," which was suggested by Hastings and Sweeney more than 40 years ago (Hastings and Sweeney, 1957; Ruoff et al., 1997). There is an infinite number of activation energies that satisfy equation 4, and nature has apparently realized some of them.

For most oscillator models, the function f is not known and numerical representation functions must be sought. A useful family of approximating functions f_{appr} is

$$P \approx f_{appr} = \tau_o \prod_i k_i^{\beta_i}, \quad (5)$$

where β_i is assumed to be temperature independent. In practice, β_i is determined numerically by calculating the oscillator's period for varying k_i, while keeping all other $k_{j\neq i}$ constant. β_i is finally determined as the slope from a log P – log k_i plot.

The above analysis shows that *any* chemical or physiological oscillator has intrinsically all necessary elements to achieve temperature compensation and that temperature compensation appears to be part of the clock mechanism.

The validity of the antagonistic balance (equation 4) has been tested for a variety of chemical oscillator models including the Brusselator, the Kauffman-Wille model, and the Oregonator (Ruoff, 1995). In all these models, temperature compensation is easily obtained, although due to the approximative nature of equation 5, a fine-tuning in activation energies is often necessary to increase the temperature range of compensation. However, calculated PRCs for temperature steps and temperature pulses of the temperature-compensated Brusselator and Kauffman-Wille models showed no agreement with experimental PRCs from circadian rhythms (Ruoff, 1994). This situation completely changed when we started to study the Goodwin model.

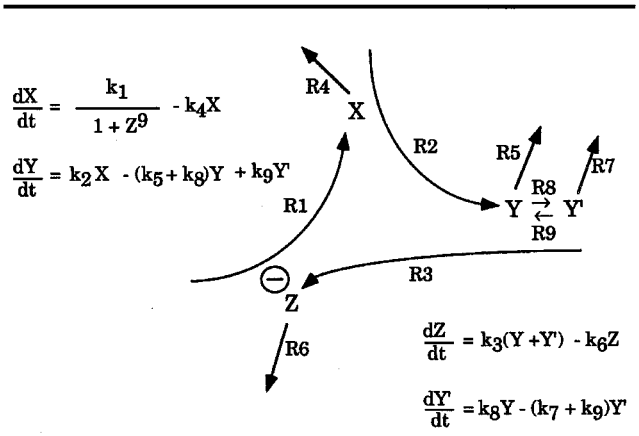

Figure 2. A version of the Goodwin model that has been used to calculate temperature behavior of *Neurospora frq* mutants and *Drosophila per* mutants. *X*, *Y*, and *Z* correspond to clock-mRNA, clock-protein, and an inhibitory factor for transcription, respectively. *Y'* is an additional form of the clock PER protein used in the *Drosophila* calculations. In the *Neurospora* calculations, the basic Goodwin oscillator has been used, that is, reactions R7-R9 have not been considered.

THE GOODWIN MODEL

The importance of negative feedback control processes started to be recognized during the 1950s. Goodwin first described a physiological oscillator model with a negative feedback loop (Goodwin, 1965; Murray, 1993). Now, more than 30 years later experimental evidence has emerged that essential elements of the circadian clock in *Neurospora* and *Drosophila* consist of negative feedback loops as considered originally by Goodwin. The importance of feedback control in circadian oscillators has also been emphasized in more general models by Johnsson and Karlsson (1972), Gander and Lewis (1979), and Lewis (1994).

Figure 2 shows a slight variation of the Goodwin model that has been used to calculate the temperature behavior of short- and long-period mutants in *Neurospora* and *Drosophila*. Not only does the Goodwin oscillator show a principally correct phasing between clock-mRNA and clock-protein, but PRCs for temperature steps and temperature pulses are similar to

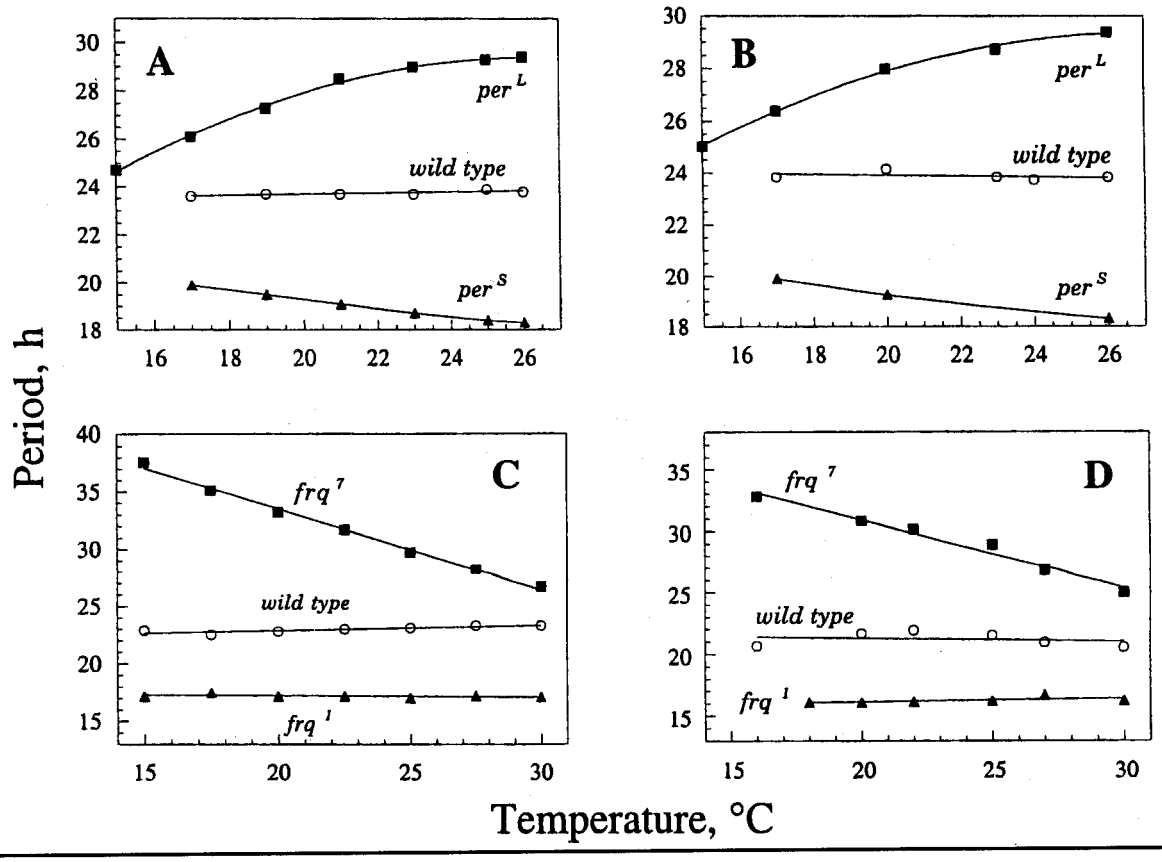

Figure 3. A. Calculated temperature behavior for *per* mutants in *Drosophila melanogaster*. E_i is the activation energy of process *Ri*. Numerical parameters: per^+: *Xo* = 1.664D-01, *Yo* = 2.458D-01, *Zo* = 1.1.455, *Yo'* = 0.0, $E_1 = 2.36 \times 10^4$ J/mol, $E_2 = 9.26 \times 10^4$ J/mol, $E_3 = 6.25 \times 10^4$ J/mol, $E_4 = 7.63 \times 10^2$ J/mol, $E_5 = 1.92 \times 10^2$ J/mol, $E_6 = 2.02 \times 10^2$ J/mol, $E_7 = E_8 = E_9 = 1.0 \times 10^2$ J/mol. At 25° C: $k_1 = k_2 = k_3 = 1.0$, $k_4 = 0.15$, $k_5 = 0.25$, $k_6 = 0.1$, $k_7 = 0.25$, $k_8 = k_9 = 1.0$. per^S: *Xo*, *Yo*, *Yo'*, and *Zo* as for per^+, $k_5 = k_7 = 0.4$ (25° C), $E_5 = 5 \times 10^4$ J/mol, other parameters as for per^+. per^L: *Xo* = 2.1D-01, *Yo* = 1.99486D-01, *Zo* = 1.99486, *Yo'* = 0.0, $k_5 = 0.3$, $k_7 = 0.15$ (25° C), $E_5 = 2.5 \times 10^4$ J/mol, $E_8 = 2.5 \times 10^5$ J/mol, $E_9 = 2.0 \times 10^4$ J/mol, other parameters as for per^+; B. Experimental results replotted from the work of Konopka et al. (1989). C. Calculated temperature behavior for *frq* mutants in *Neurospora crassa*. Numerical parameters: *wild-type*, frq^+: $E_1 = 2.36 \times 10^4$ J/mol, $E_2 = 9.26 \times 10^4$ J/mol, $E_3 = 6.25 \times 10^4$ J/mol, $E_4 = 7.63 \times 10^2$ J/mol, $E_5 = 1.92 \times 10^2$ J/mol, $E_6 = 2.02 \times 10^2$ J/mol. At 25° C: $k_1 = k_2 = k_3 = 1.0$, $k_4 = k_5 = 0.2$, $k_6 = 0.1$, $k_7 = k_8 = k_9 = 0.0$. frq^1: $k_5 = 0.5$ (25° C, shows damped oscillations), $E_5 = 1.92 \times 10^2$ J/mol, other parameters as for *wild type*. frq^7: $k_5 = 0.1$ (25° C), $E_5 = 5.0 \times 10^4$ J/mol, other parameters as for frq^+. D. Experimental results replotted from the work of Gardner and Feldman (1981).

what has been experimentally observed (Ruoff and Rensing, 1996).

Temperature Behavior of Clock Mutants

An interesting feature of the Goodwin model is that the period depends on the degradation reactions R4, R5, and R6, while the anabolic reactions R1, R2, and R3 have practically no influence on the period (Ruoff et al., 1997). By decreasing one of the rate constants of the degradation reactions (k_5), temperature compensation is lost and the response is similar to that observed in the *N. crassa* frq^7 mutant. In fact, the temperature behavior of the long- and short-period mutants of *frq* in *N. crassa* and of *per* in *Drosophila* can be understood in terms of degradation of the clock protein or the corresponding clock mRNA (Ruoff et al., 1996). According to the Goodwin model, the short-period mutants (frq^1, per^S) are related to a rapid degradation of the clock-protein or clock-mRNA, while in long-period mutants the clock-protein (or clock-mRNA) is degraded more slowly. To simulate per^L's temperature behavior (Fig. 3), a temperature-dependent equilibrium between two forms of the clock-protein (Y', Y) has to be considered: At higher temperatures, the equilibrium between Y and Y' is shifted to the side of the slower degrading protein species Y'.

Cycloheximide PRCs in *N. crassa*

The long-period mutant frq^7 is known to be less sensitive to perturbations by cycloheximide (CHX) pulses

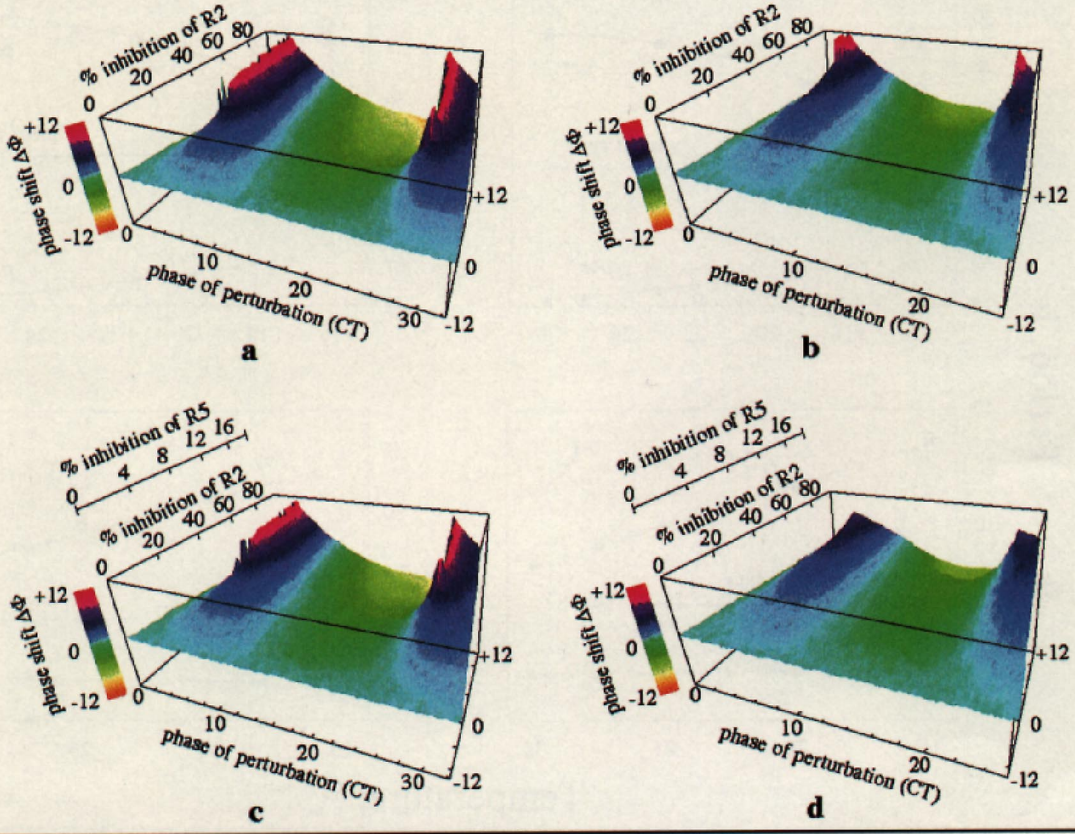

Figure 4. Effect of inhibitory pulses (1-time unit duration) on *Neurospora crassa* wild-type (a, c) and *frq*^{7} (b, d) parameterizations in the Goodwin model. Φ is the phase of perturbation (0-30 time units) and ΔΦ is the phase shift (–12 to +12 time units). The inhibition axis indicates an increased linear and simultaneous inhibition of reactions R2 and R5 from 0% to 98%, and from 0% to 20%, respectively. For details, see Ruoff et al. (1999a). As shown by experiments, the *frq*^{7}-parameterization (b, d) is clearly less affected by inhibitory (CHX) pulses.

(Dunlap and Feldman, 1988) when compared with wild-type (*frq*$^+$) resetting. We have tested whether the *frq*$^+$ and the *frq*^{7} parametrization of the Goodwin model (Table 1) would be able to describe this behavior. Indeed, the effect of CHX pulses can be simulated by the Goodwin model when using a strong inhibitory pulse on process R2 accompanied by a simultaneous slight inhibitory pulse on reaction R5. Figures 4b and d show that the Goodwin *frq*^{7} parameterization is clearly less affected by such inhibitory pulses compared with the wild-type parameterization (Fig. 4 a,c).

frq-mRNA Levels

We are beginning to investigate *frq*-mRNA levels in the wild-type (*bd*) and in the *frq*^{7}-mutant by RT-PCR. The first results show that at peak times the *frq*-mRNA level is significantly higher in the *frq*^{7} mutant compared to the wild-type strain (Fig. 5). A higher amplitude of *frq*-mRNA oscillations in *frq*^{7} was already observed by Aronson et al. (1994). Model calculations

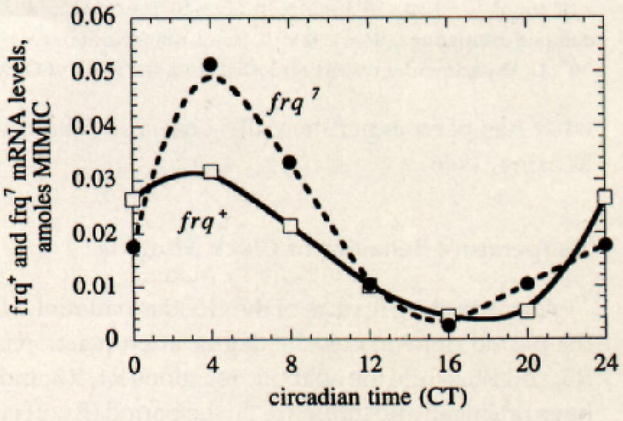

Figure 5. Comparison between experimentally determined *frq*$^+$-mRNA and *frq*^{7}-mRNA levels by RT-PCR (each point is the mean of 2 independent experiments). Although we still consider these results as preliminary, they are in contrast to the predicted mRNA levels of *frq*^{7} and *frq*$^+$-parameterizations in the Goodwin model, where *X* from *frq*$^+$-parameterization oscillates at a 2 times higher level than *X* from *frq*^{7}-parameterization.

show that these results are not consistent with the Goodwin oscillator, which predicts that *frq*-mRNA oscillations in the wild type occur at a level 2 times higher than the level in the *frq*^{7}-mutant (data not shown).

AN ALTERNATIVE FORMULATION OF INHIBITION

This discrepancy between experimental *frq*$^+$/*frq*^{7}-mRNA levels and those simulated by the Goodwin model prompted us to look for an alternative formulation of inhibition. One possibility that accounts for the more relaxational type of *frq*-mRNA oscillations in *N. crassa* is the introduction of critical inhibitor concentrations Z_{max} and Z_{min}, which determine when transcription inhibition is switched on and when it is turned off. In its simplest version (Fig. 6A), transcription of the *frq* gene is inhibited whenever Z becomes larger than Z_{max}. On the other hand, transcription is restored when Z falls below a lower critical value Z_{min}. A consequence of such a relaxational inhibition scheme is that clock-mRNA and clock-protein start to increase almost simultaneously, while the phase difference between the minima of clock mRNA and clock protein, which occurs in the original Goodwin model, is lost. In fact, experimental results (Fig. 6 B,C) indicate precisely this behavior.

ESTIMATING *frq*-mRNA AND FRQ-PROTEIN DEGRADATION RATE CONSTANTS

If we assume that the inhibitory scheme in Figure 6A is operative in the *Neurospora* clock, an attempt to estimate the degradation rate constants for *frq*-mRNA and FRQ-protein from the available experimental results (Fig. 5; Fig. 6 B, C) can be made.

In the first step, the *frq*-mRNA (X) degradation rate constant k_4 is determined assuming that reaction R1 is off and $k_1 = 0$ (Fig. 7A). In this case, X decreases exponentially by a one-order process, which is described by the rate equation $X(t) = X_{start} \exp(-k_4 t)$. Both our experimental results (Fig. 5) and those by Garceau et al. (1997) (Fig. 6 B, C) show that the *frq*-mRNA decay can be described quite well by such a process. Table 2 summarizes the degradation rate constants obtained for *frq*$^+$ and *frq*^{7}-mRNAs.

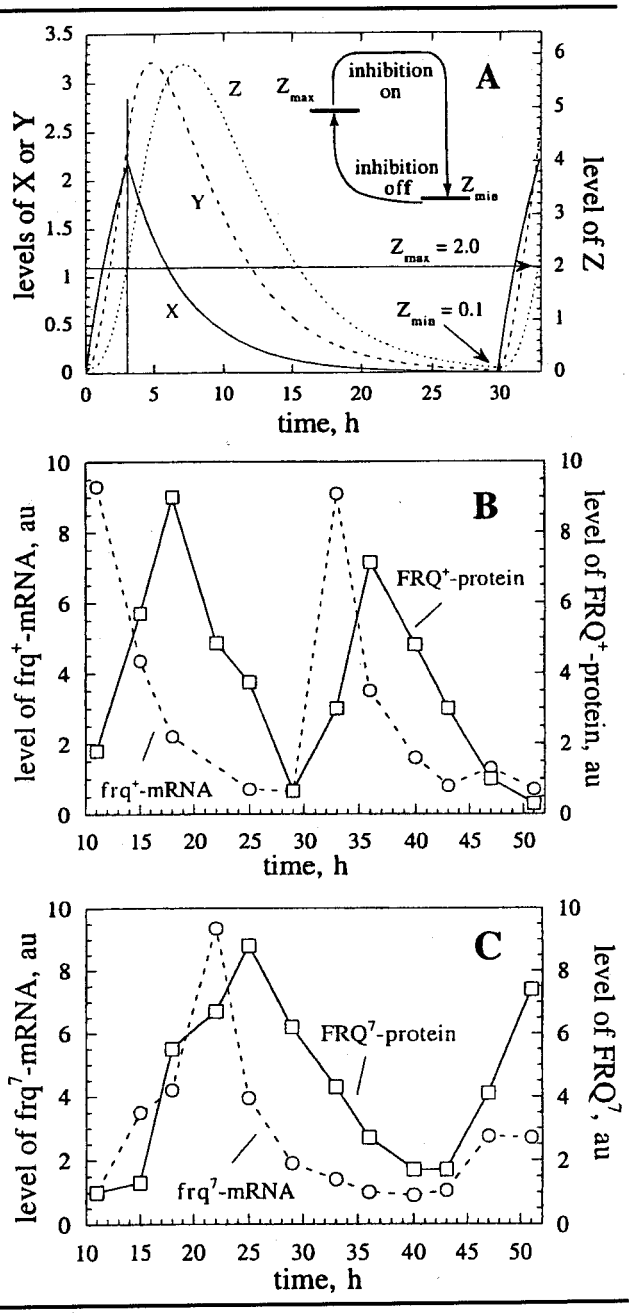

Figure 6. A. A threshold inhibition scheme proposed for the *Neurospora* circadian clock. Z_{max} determines the Z level when transcription inhibition occurs ($k_1 = 0$), while Z_{min} determines the phase when transcription is restored ($k_1 > 0$). B, C. Experimental *frq*-mRNA and FRQ-protein levels for wild type (*frq*$^+$) and the long-period mutant *frq*^{7}, which indicate their practically simultaneous increase at the beginning of the cycle (Replotted from the work of Garceau et al., 1997).

In the second step, FRQ-protein degradation for wild-type and for the *frq*^{7}-mutant can be estimated by two ways, either (a) by a direct exponential fit of the

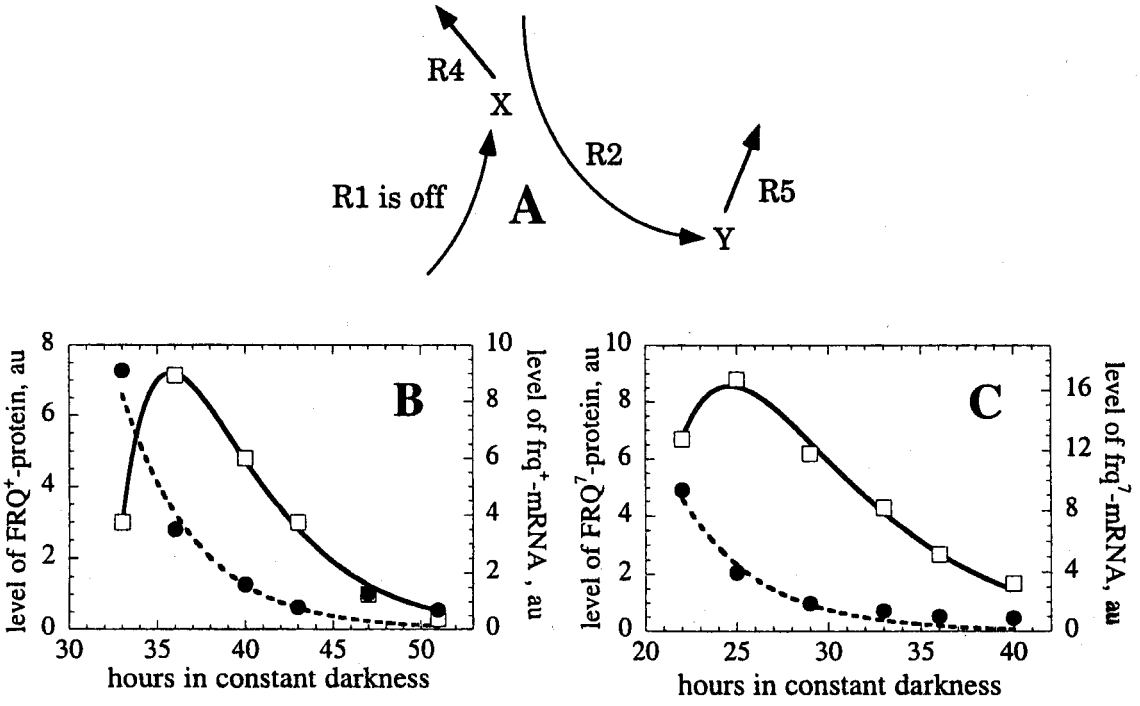

Figure 7. A. Reaction scheme for determining *frq*-mRNA degradation rate constant k_4 and FRQ-protein degradation rate constant k_5. B, C. Fit of 1-order process (dashed lines) to experimental *frq*-mRNA data (solid circles) and fit of the sequential processes R2 and R5 (solid lines) to experimental FRQ-protein data (open squares). The rate constant values are those given in Table 2.

declining FRQ-protein levels or (b) by fitting the function

$$Y(t) = Y_{start}\exp(-k_5 t) + \frac{k_2 X_{start}}{k_5 - k_4}\left(\exp(-k_4 t) - \exp(-k_5 t)\right) \quad (6)$$

to the increasing and decreasing FRQ levels and taking into account that FRQ-protein is still produced in the presence of *frq*-mRNA. Equation 6 is the solution of the rate equation $\frac{dY}{dt} + k_5 Y = k_2 X_{start}\exp(-k_4 t)$, which assumes an exponential decay in X (R1 transcription is off, i.e., $k_1 = 0$), while Y is formed by reaction R2 and degraded by process R5 (with rate constants k_2 and k_5, respectively). X_{start} and Y_{start} represent the initial values of X and Y, respectively. In our calculation, we have used the peak value of X and the corresponding Y value as starting points. We allowed to vary k_2 and k_5 freely to fit equation 6 to the experimental FRQ$^+$ and FRQ^7-protein data (Fig. 7 B,C). Both methods (a) and (b) indicate that the FRQ^7-degradation rate constant is smaller (approximately by a factor of 2) than the degradation rate constants of the wild-type FRQ-protein (Fig. 7, Table 2). In fact, the range of these rate constant values fits very well to our previously (Ruoff et al., 1996) assumed rate constant values (Table 1).

DISCUSSION

Are Degradation Processes Important in the *Neurospora* Clock?

The results shown in Figure 7 and Table 2 agree with the earlier predictions (Ruoff and Rensing, 1996; Ruoff et al., 1996) of the Goodwin model that long-period mutants may be characterized by a slower degradation rate of either clock-mRNA or clock-protein as compared to the wild-type. Despite these encouraging results, one should still remain cautious. First of all, none of the experiments so far was explicitly designed for determining either *frq*-mRNA or FRQ-protein degradation rates. Additional experiments are needed to estimate *frq*-mRNA and FRQ-protein degradation rates—especially in the presence of transcription or translation inhibitors, respectively.

Another important question is whether the higher *frq*^{7}-mRNA levels are related to a less effective transcription inhibition by FRQ^7 (or FRQ^7-phosphorylated forms). A similar relationship between *frq*-mRNA lev-

Table 2. Estimated 1-order rate constants for frq^+/frq^7-mRNA and FRQ^+/FRQ^7-protein degradation[a]

Species	*Rate Constant, h^{-1}*	*Rate Constant, h^{-1}*
frq^+-mRNA	$k_4 = 0.237$ ($R = 0.992$)[b]	
	$k_4 = 0.170$ ($R = 0.980$)[d]	—
frq^7-mRNA	$k_4 = 0.225$ ($R = 0.993$)[b]	
	$k_4 = 0.263$ ($R = 0.9994$)[d]	—
FRQ^+-protein[b]	$k_5 = 0.256$ ($R = 0.984$)[c]	$k_2 = 0.546$ $k_4 = 0.237$ $k_5 = 0.355$ ($R = 0.997$)[e]
FRQ^7-protein[b]	$k_5 = 0.111$ ($R = 0.994$)[c]	$k_2 = 0.318$ $k_4 = 0.225$ $k_5 = 0.192$ ($R = 0.996$)[f]

a. Species half-life $= \dfrac{\ln 2}{\text{rate constant}}$.

b. From replots of Garceau et al. (1997) data.
c. Simple exponential fit. Presence of *frq*-mRNA neglected.
d. From Figure 5.
e. Presence of frq^+-mRNA taken into account. See Figure 7B for details.
f. Presence of frq^7-mRNA taken into account. See Figure 7C for details.

els and the functionality of the FRQ-protein was found in the frq^9 strain (Merrow et al., 1997). In frq^9, *frq*-mRNA is at a high level, because no functional FRQ is made. If the higher frq^7-mRNA level is related to a less effective FRQ-protein (leading to a higher Z_{max} threshold), then an increase in Z_{max} may not only explain a higher frq^7-mRNA level but would also lead to an increase in period length independent of degradation processes.

Luo et al. (1998) found that the FRQ-protein rapidly enters the nucleus and that degradation of FRQ in the nucleus has a similar time-scale as *frq*-mRNA degradation in the cytoplasma. In view of the threshold model, the rapid appearance of FRQ in the nucleus seems to ensure a rapid inhibition of transcription. On the other hand, the period length appears to be correlated to the cytosolic FRQ, which is degraded at a somewhat slower time scale: As long as sufficent cytosolic FRQ is transported into the nucleus, inhibition may remain. However, once the cytosolic FRQ is too low, the inhibitory FRQ level in the nucleus may be driven below Z_{min} such that transcription can start again. In this view, FRQ-degradation in the cytosol appears to be an important determinant of *Neurospora*'s circadian period. It would be of importance to explicitly determine the degradation rates of cytosolic FRQ and FRQ inside the nucleus both for wild-type and for several of the *frq* mutants.

Inhibition Threshold and Phase-Resetting Behavior

The threshold concept of inhibition alters completely the phase-resetting behavior: While the original Goodwin oscillator (and probably also the other models that have a Hill-type inhibition [Leloup and Goldbeter, 1997, 1998; Hong and Tyson, 1997; Olde Scheper et al., 1999]), show a soft resetting (i.e., transient phase shifts occur during each cycle of resetting), the threshold model of inhibition leads to an immediate resetting. This can explain differences in resetting between the "soft" *Drosophila* resetting behavior (Zimmerman et al., 1968) and the "hard" (immediate) resetting observed in *N. crassa* (Lakin-Thomas et al., 1990). In fact, the *per*-mRNA and PER-protein oscillations are consistent with the Hill-type inhibition, as indicated by the phase difference between minimum *per*-mRNA and PER-protein (Zeng et al., 1994).

Occam's Razor: On the Importance of Minimal Models

The Goodwin model (Fig. 2) has to be considered as a *minimal* model, that is, it is considered to contain only the most important elements of the circadian clock. Models with similar dynamics as the Goodwin oscillator have been described by Christensen et al. (1984), Lewis (1994), and Olde Scheper et al. (1999). In the 2-variable model by Olde Scheper et al. (1999), the unrealistic high Hill coefficient in the inhibition term of the original Goodwin oscillator was reduced from 9 to 2; however, this was done at the expense of an increased reaction order in the protein synthesis process.

More detailed oscillator models for the *Drosophila* clock based on a negative feedback have recently been described by Leloup and Goldbeter (1997, 1998) and

Hong and Tyson (1997). These models emphasize the importance of phosphorylation reactions or the entry kinetics of the PER protein into the nucleus.

One should be aware, however, that as the number of adjustable parameters increases in a model, the general performance to describe certain experimental data sets may increase, but the predictive power may still be low. It appears important, therefore, that the development or refinement of a model is aimed at finding experimentally testable numerical values of parameters—preferably in relation to a minimum model. What is a minimum model? Minimum models are the remains of Occam's razor:[1] A model should not increase beyond what is necessary; that is, the number of adjustable parameters should not increase beyond what is required to explain something, and no more assumptions should be made than are minimally needed. The practical problem of applying Occam's razor is to decide which of the considered (or established) processes are necessary and which are not. This may not be an easy task, as it requires a priori knowledge about the clock mechanism itself. Nevertheless, minimal models are important, because they serve as "nuclei" in the construction of more detailed models.

While this paper was in press, site directed mutagenesis experiments by Liu, Loros, and Dunlap show that phosphorylation of the *Neurospora* clock protein determines its turnover rate and the period length of the circadian clock. Interestingly, mutation at Ser 513 leads to a dramatic reduction of the rate of FRQ degradation and to a very long (31 h) period (to appear in Proc Natl Acad Sci USA; J. Dunlap, personal communication).

NOTE

1. "Plurality is not to be assumed without necessity." William of Occam, c. 1285, d.c. 1349.

REFERENCES

Aronson BD, Johnson KA, Loros JJ, and Dunlap JC (1994) Negative feedback defining a circadian clock: Autoregulation of the clock gene *frequency*. Science 263:1578-1584.

Christensen ND, Lewis RD, and Gander PH (1984) Properties of a feedback model for the circadian clock of *Hemideina thoracica* (Orthoptera; Stenopelmatidae). Biol Cybern 51:87-92.

Dunlap JC and Feldman JF (1988) On the role of protein synthesis in the circadian clock of *Neurospora crassa*. Proc Natl Acad Sci U S A 85:1096-1100.

Edmunds LN (1988) *Cellular and Molecular Bases of Biological Clocks*, Springer-Verlag, New York.

Gander PH and Lewis RD (1979) The circadian locomotor rhythm of *Hemideina thoracica* (Orthoptera): The effects of temperature perturbations. Int J Chronobiol 6:243-62.

Garceau NY, Liu Y, Loros JJ, and Dunlap JC (1997) Alternative initiation of translation and time-specific phosphorylation yield multiple forms of the essential clock protein FREQUENCY. Cell 89:469-476.

Gardner GF and Feldman JF (1981) Temperature compensation of circadian period length in clock mutants of *Neurospora crassa*. Plant Physiol 68:1244-1248.

Goodwin BC (1965) Oscillatory behavior in enzymatic control processes. In *Advances in Enzyme Regulation*, Vol. 3, G Weber, ed, pp 425-438, Pergamon, Oxford, UK.

Hastings JW and Sweeney BM (1957) On the mechanism of temperature independence in a biological clock. Proc Natl Acad Sci U S A 43:804-811.

Hindmarsh AC (1980) LSODE and LSODI, two new initial value ordinary differential equation solvers. ACM-SIGNUM Newsletter 15:10-11.

Hong CI and Tyson JJ (1997) A proposal for temperature compensation of the circadian rhythm in *Drosophila* based on dimerization of the PER protein. Chronobiol Int 14:521-530.

Johnsson A and Karlsson HG (1972) A feedback model for biological rhythms. Mathematical description and basic properties of the model. J Theor Biol 36:153-174.

Kippert F (1997) The ultradian clocks of eukaryotic microbes: Timekeeping devices displaying a homeostasis of the period. Chronobiol Int 14:469-480.

Kondepudi D and Prigogine I (1998) *Modern Thermodynamics: From Heat Engines to Dissipative Structures*, John Wiley, New York.

Konopka R, Pittendrigh CS, and Orr D (1989) Reciprocal behavior associated with altered homeostasis and photosensitivity of *Drosophila* clock mutants. J Neurogenet 6: 1-10.

Laidler KJ (1972) Unconventional applications of the Arrhenius law. J Chem Educ 49:343-344.

Laidler KJ and Peterman BF (1979) Temperature effects in enzyme kinetics. Methods Enzymol 63A:234-257.

Lakin-Thomas PL, Coté GG, and Brody S (1990) Circadian rhythms in *Neurospora crassa:* Biochemistry and genetics. Crit Rev Microbiol 17:365-416.

Leloup J-C and Goldbeter A (1997) Temperature compensation of circadian rhythms: Control of the period in a model for circadian oscillations of the PER protein in *Drosophila*. Chronobiol Int 14:511-520.

Leloup J-C and Goldbeter A (1998) A model for circadian rhythms in *Drosophila* incorporating the formation of a complex between PER and TIM proteins. J Biol Rhythms 13:70-87.

Lewis RD (1994) Modelling the circadian system of the weta, *Hemideina thoracica* (Orthoptera: Stenopelmatidae). J R Soc New Zealand 24:395-421.

Luo C, Loros JJ, and Dunlap JC (1998) Nuclear localization is required for function of the essential clock protein FRQ. EMBO J 17:1228-1235.

Merrow MW, Garceau NY, and Dunlap JC (1997) Dissection of a circadian oscillation into discrete domains. Proc Natl Acad Sci U S A 94:3877-3882.

Murray JD (1993) *Mathematical Biology*, Springer-Verlag, Berlin.

Noyes RM (1986) Kinetics and mechanisms of complex reactions. In *Investigations of Rates and Mechanisms*, CF Bernasconi, ed, pp 373-423, John Wiley, New York.

Olde Scheper T, Klinkenberg D, Pennartz C, and van Pelt J (1999) A mathematical model for the intracellular circadian rhythm generator. J Neurosci 19:40-47.

Pittendrigh CS (1993) Temporal organization: Reflections of a Darwinian clock-watcher. Annu Rev Physiol 55:17-54.

Ruoff P (1992) Introducing temperature compensation in any reaction kinetic oscillator model. J Interdiscipl Cycle Res 23:92-99.

Ruoff P (1994) Phase resetting by temperature perturbations in the temperature compensated Brusselator and Kauffman-Wille models. Working Papers from Stavanger College [ISSN: 0801-5872], No. 198, Stavanger College, Stavanger, Norway.

Ruoff (1995) Antagonistic balance in the Oregonator: About the possibility of temperature compensation in the Belousov-Zhabotinsky reaction. Physica D 84:204-211.

Ruoff P, Mohsenzadeh S, and Rensing L (1996) Circadian rhythm and protein turnover: The influence of temperature on the period lengths of clock mutants simulated by the Goodwin oscillator. Naturwissenschaften 83:514-517.

Ruoff P and Rensing L (1996) The temperature compensated Goodwin model simulates many circadian clock properties. J Theor Biol 179:275-285.

Ruoff P, Rensing L, Kommedal R, and Mohsenzadeh S (1997) Modelling temperature compensation in chemical and biological oscillators. Chronobiol Int 14:499-511.

Ruoff P, Vinsjevik M, Mohsenzadeh S, and Rensing L (1999a) The Goodwin model: Simulating the effect of cycloheximide and heat shock on the sporulation rhythm of *Neurospora crassa*. J Theor Biol 196:486-494.

Ruoff P, Vinsjevik M, and Rensing L (1999b) Temperature compensation in biological oscillators: A challenge for joint experimental and theoretical analysis. Comments on Theoretical Biology (in press).

Siebert PD and Kellogg DE (1995) PCR MIMICs: Competitive DNA fragments for use in quantitative PCR. In *PCR 2*, MJ McPherson, BD Hames, and GR Taylor, eds, pp 135-148, Oxford University Press, New York.

Vogel HA (1956) A convenient growth medium for *Neurospora* (medium M). Microbiol Gen Bull 15:42-43.

Winfree AT (1980) *The Geometry of Biological Time*, Springer-Verlag, New York.

Zimmerman WF, Pittendrigh CS, and Pavlidis T (1968) Temperature compensation of the circadian oscillation in *Drosophila pseudoobscura* and its entrainment by temperature cycles. J Insect Physiol 14:669-684.